Electronic stopping of swift partially stripped molecules and clusters

J. Jensen and P. Sigmund
*Physics Department, SDU Odense University, DK-5230 Odense M, Denmark**
and Laboratoire des Solides Irradiés, CEA/Ecole Polytechnique, F-91128 Palaiseau, France
(Received 16 February 1999; revised manuscript received 28 June 1999; published 16 February 2000)

The electronic stopping power of a material for swift molecules or clusters need not be an incoherent superposition of the stopping powers for the constituent atomic ions. However, only the stopping of hydrogen clusters is understood theoretically. Experimental results indicate that effects due to coherent stopping are smaller for heavier molecules and clusters, and occasionally destructive interferences were found experimentally when constructive interferences were expected. The present theoretical study aims at differences between the stopping of hydrogen and heavier clusters. The role of projectile screening is emphasized, and explicit estimates are presented for coherent-stopping effects due to target excitation or ionization. The importance of a proper description of target resonances is pointed out. As expected, projectile screening reduces the significance of coherent stopping. Competing effects such as projectile excitation or ionization, variations in charge-state and charge-dependent stopping, and the clearing-the-way effect are discussed qualitatively. The main focus is on randomly oriented beams, but attention is also given to stopping of aligned molecules.

PACS number(s): 34.50.Bw, 36.40.−c, 52.40.Mj

I. INTRODUCTION

Beams of molecule and cluster ions covering a wide range of energies have become available recently. Such beams are useful tools in fundamental research on the interaction of particles with matter, expanding the number of available degrees of freedom and thus the range of observable phenomena. Moreover, there are promising applications in science and technology. Cluster beams with energies per atom in the keV or MeV range allow deposition of energy in matter at densities far above what can be achieved with beams of atomic ions [1,2]. This has implications on ion-beam-induced desorption [3,4], track formation [5], and inertial confinement fusion [6]. Conversely, clusters with energies per atom in the eV regime are of potential use for depositing material because of high achievable particle currents combined with low damage rates [7,8].

The present study concerns the deposition of electronic energy by swift molecules and clusters in matter, where ''swift'' refers to projectile speeds above the Bohr velocity v_0. For a survey of current knowledge the reader is referred to a recent summary [9].

A central quantity characterizing the interaction of swift ionized clusters with matter is the mean energy loss per traveled path length, or stopping power. This quantity is conventionally approximated by the sum of the stopping powers for the constituent atomic ions of the cluster,

$$\left(\frac{dE}{dx}\right)_{\text{cluster}} \cong \sum_{\text{cluster}} \left(\frac{dE}{dx}\right)_{\text{atom}}. \tag{1}$$

Such a relationship assumes a short range of the interactions giving rise to energy transfer from the cluster to the target: If the internuclear distance in a cluster exceeds the interaction range for events that lead to significant energy transfer, the cluster-target interaction may be viewed as an incoherent superposition of ion-atom collisions.

Equation (1), while by no means an exact relationship, is well established as a first approximation. Deviations—summarized under the heading of ''coherent stopping''—have been identified primarily for swift ions: The interaction range for Coulomb excitation of a given target resonance frequency ω_0 is given by Bohr's adiabatic radius,

$$a_{\text{ad}} = \frac{v}{\omega_0}, \tag{2}$$

where v is the projectile speed. At sufficiently high speed this quantity can exceed internuclear distances r_{ij} in a cluster and thus cause interferences which may show up as coherent stopping. Both constructive and destructive interferences are known [9].

Rather few measurements have been performed to determine the significance of coherent stopping and only quite small deviations from Eq. (1) have been found. Conversely, the theoretical literature is extensive and quite drastic coherency effects have repeatedly been predicted. It is the main goal of this paper to track the origin(s) of this apparent discrepancy. At the same time we point at other potential sources of coherent stopping, some of which have not been discussed previously in this context. We also provide revised estimates of electronic stopping by target excitation, i.e., the process that is generally considered dominant and the only one for which estimates are available in the literature. We note that most of the theoretical literature explicitly or implicitly refers to light-atom clusters, in particular hydrogen clusters. For several reasons such estimates do not directly apply to clusters made up of heavier ions which we address in the present paper.

The possibility of a major enhancement in stopping power was suggested by a heavily oversimplified argument, the main weakness of which was pointed out right away by those authors who brought it forward [10]. It is based on the qua-

*Address for correspondence.

 ©2000 The American Physical Society

dratic dependence of the stopping power for a point charge on its atomic number Z_i. In a united-atom picture, one might view a penetrating cluster as a point charge $\Sigma_i Z_i e$. Then the stopping power could be $\propto(\Sigma_i Z_i)^2$, which exceeds the sum of atomic stopping powers ($\propto\Sigma_i Z_i^2$). The ratio between the two quantities, the enhancement factor

$$R=\frac{(dE/dx)_{\text{cluster}}}{\Sigma_{\text{cluster}}(dE/dx)_{\text{atom}}}, \tag{3}$$

could then become as large as $R\simeq n$ for an n-atomic cluster. In contrast, even for large clusters, measured enhancements have always been below a factor of 1.5 and rarely more than ~20% above unity [10–16].

The above argument neglects the vectorial nature of the electric fields originating in the projectile charges. There is a sizable contribution from close collisions to electronic stopping, for which the electric fields originating in cluster atoms tend to cancel so that the united-atom picture breaks down. Such destructive interference may in fact cause negative enhancement in stopping power at low projectile speed, as was realized early on [10] and confirmed experimentally [13].

Clusters are typically not completely stripped of their electrons, in particular, in the initial parts of their trajectories through the stopping medium. For an incompletely stripped cluster the contribution from long-range interactions to stopping is reduced more or less dramatically. As a consequence, coherent stopping loses significance. This is especially pronounced for clusters that consist of atoms heavier than hydrogen since the screening radius decreases with increasing atomic number. As a consequence, coherent stopping must be less pronounced in heavier clusters. Ignoring this feature leads to drastically overestimated coherency effects. A recent example is Ref. [17] where enhancement factors up to $R\sim5$ were predicted for accelerated C_{60} molecules, in sharp contrast with existing but unquoted experimental data [14].

A more subtle but no less relevant point concerns the description of the stopping medium, for which most often a homogeneous electron gas characterized by a plasma frequency ω_P has been adopted. Plasma resonances in solids lie in the 10–20 eV range and hence contribute to stopping within rather large adiabatic radii v/ω_P. Consequently, significant coherent stopping is expected at high and moderate projectile speeds. However, with increasing v, inner target electrons also contribute to stopping, albeit over a smaller interaction radius and hence mostly affecting incoherent stopping. Thus the relative significance of coherent stopping decreases. Even though this point was recognized occasionally [18,19] it has more often been overlooked.

Projectile screening and target description are asserted to be the most significant reasons why numerous theoretical estimates tend to overestimate coherent stopping. However, other effects come into play in the theory of heavy-ion stopping and, hence, need to be considered in context. In the velocity range accessible to cluster beams we need to mention projectile excitation or ionization, charge equilibration and equilibrium charge states, energy loss by charge exchange, and nonlinear stopping. We shall argue that none of these effects should lead to drastically enhanced stopping powers, but both positive and negative enhancements may be expected and would need to be estimated if precise data for molecule and cluster stopping were needed for fundamental or practical reasons. We see no such need at present and, therefore, put emphasis on dominant processes.

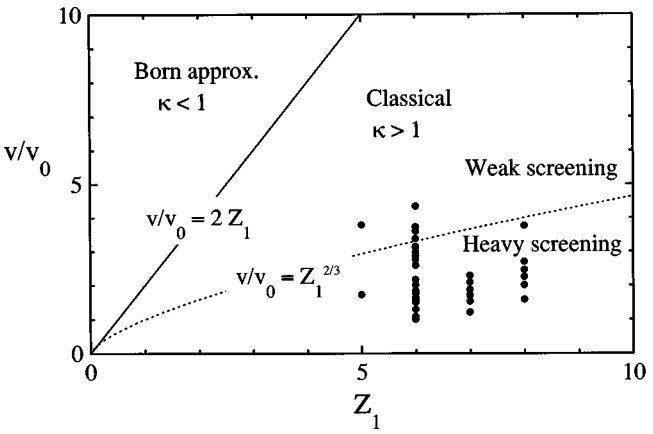

FIG. 1. Regimes of validity of Born approximation and classical-orbit picture, and regimes of stripped and dressed ions in charge-state equilibrium. Points refer to bombardment parameters in reported measurements on cluster stopping for $Z_1>1$. This is a modified version of a graph in Ref. [55].

In passing on we mention that internuclear distances in clusters change during passage through a target because of Coulomb explosion and multiple scattering. This effect, causing coherence effects to vary—generally to decrease—with traveled path length or increasing target thickness [10,12,13], is only weakly related to the fundamental problem of coherent stopping but complicates the analysis of experiments and, therefore, cannot be disregarded. It also sets severe limits on potential applications of stopping-power enhancement in attempts to achieve high-energy deposition density.

II. PRELIMINARIES

A. Classical and quantal stopping theory

For atomic ions the regime of classical stopping theory is defined by the Bohr criterion [20]

$$\kappa=\frac{2Z_1v_0}{v}>1, \tag{4}$$

where Z_1 is the atomic number and $v_0=e^2/\hbar$ the Bohr velocity. In the opposite case, quantal perturbation theory [21,22] applies. Equation (4) likewise governs the incoherent stopping of clusters. The relation is illustrated in Fig. 1 [55]. Experimental parameters for reported measurements on cluster stopping with $Z_1>1$ have been included [12,14–16,23]. It is seen that these data fall into the classical regime.

The most common description of cluster stopping is based on Lindhard's quantal dielectric theory for a point charge moving through a homogeneous free electron gas [22], adapted to a group of point charges by Arista [24]. Figure 1 suggests that such a picture is valid for hydrogen clusters for

$v > 2v_0$, but a classical treatment should be more appropriate for atomic ions heavier than hydrogen. Classical treatments for bare cluster ions have been reported in Refs. [25, 26].

Coherence effects involve more than one target atom at a time and hence refer to large impact parameters. Quantal perturbation theory in the impact-parameter picture yields results equivalent to the Bohr model in that limit [27]. Therefore, the result of the theoretical treatment of coherent stopping is insensitive to the choice between a classical and a quantal picture.

The same statement is not true, however, for incoherent stopping, i.e., stopping of individual atomic ions. Hence, if the enhancement factor *R*, Eq. (3), is rewritten in the form

$$R = 1 + \frac{\delta(dE/dx)_{\mathrm{coh}}}{(dE/dx)_{\mathrm{incoh}}}, \tag{5}$$

where $\delta(dE/dx)_{\mathrm{coh}} = (dE/dx)_{\mathrm{cluster}} - \Sigma(dE/dx)_{\mathrm{atom}}$, it is the *denominator* rather than the numerator that is sensitive to the choice between a classical and a quantal treatment. Far away from the crossover ($\kappa \simeq 1$) the difference may be substantial (examples to be given below).

B. Screening

For atomic ions in charge-state equilibrium, significant projectile screening is expected for [20]

$$v \lesssim Z_1^{2/3} v_0. \tag{6}$$

Equation (6) has also been included in Fig. 1. It is seen that most reported experimental data for heavier cluster species fall into the regime of heavy screening.

Measured stopping powers do not necessarily refer to charge equilibrium. For swift clusters the incident charge is most often below equilibrium. Hence, screening effects tend to be even more pronounced in preequilibrium.

For partially stripped ions the effective projectile charge responsible for stopping depends on the impact parameter, approaching the nuclear charge $Z_1 e$ at small and the ion charge $q_1 e$ at large impact parameters. Incoherent stopping receives contributions from both close and distant interactions while coherent stopping originates in more distant interactions which get less significant in the presence of screening. This causes coherence effects to decrease with increasing screening.

Note that according to Fig. 1 the regime of significant screening lies in the classical regime.

III. SCREENING AND TARGET EXCITATION

The present section provides estimates of the effect of screening on coherent stopping by target excitation or ionization. The effect is treated on the basis of both classical and quantal stopping theory. Equivalent results must be expected for the coherence correction δS according to the discussion in Sec. II A. For incoherent stopping of heavy-ion clusters a classical treatment is most appropriate. Reference will here be made to a recent treatment of charge-dependent stopping of swift atomic ions [28].

A. Bohr stopping of screened clusters

In the Bohr theory, distant interactions are described by a time-dependent electric field acting on a classical electron bound harmonically to the origin with a resonant frequency ω_0. The energy transfer is given by

$$T = \frac{1}{2m} \left| \int_{-\infty}^{\infty} dt\, \mathbf{F}(t) e^{-i\omega_0 t} \right|^2. \tag{7}$$

Here the force is determined by $\mathbf{F}(t) = -\nabla \Sigma_i V_i(\mathbf{r} - \mathbf{R}_i(t))$, where $\mathbf{r}$ denotes the electron coordinate and $\mathbf{R}_i = \mathbf{p} + \mathbf{v}t + \mathbf{r}_i$ the trajectory of the ith projectile nucleus in uniform motion. $\mathbf{p}$ and $\mathbf{v}$ denote the impact parameter and velocity, respectively, for the center of mass of the projectile. To the lowest order in $\mathbf{r}$ (dipole approximation), Eq. (7) yields

$$\begin{aligned} T = \frac{2\pi^2}{m} \sum_{ij} \int d^3\mathbf{k} \int d^3\mathbf{k}'\, V_i^*(\mathbf{k}) V_j(\mathbf{k}')(\mathbf{k}\cdot\mathbf{k}') \\ \times e^{i\mathbf{k}\cdot\mathbf{r}_i - i\mathbf{k}'\cdot\mathbf{r}_j} e^{i(\mathbf{k}-\mathbf{k}')\cdot\mathbf{p}} \\ \times \delta(\omega_0 + \mathbf{k}\cdot\mathbf{v})\, \delta(\omega_0 + \mathbf{k}'\cdot\mathbf{v}), \end{aligned} \tag{8}$$

where $\delta(\cdots)$ denotes the Dirac function. We may split the energy transfer according to

$$T = T_0 + \delta T, \tag{9}$$

where T_0 comprises the terms for $i = j$ in the double sum, i.e., the sum of stopping powers for independent atomic ions which make up the contribution from incoherent stopping. The terms for $i \neq j$ then make up the correction δT for coherent stopping. For the further analysis of T_0 we refer to Ref. [28]. Presently the focus will be on δT.

Although Eq. (8) has been derived for large impact parameters, let us integrate it over all $\mathbf{p}$ to obtain a first estimate of the coherence correction to the stopping cross section

$$\begin{aligned} \delta S &= \int d^2\mathbf{p}\, \delta T \\ &= \frac{8\pi^4}{mv} \sum_{i \neq j} \int d^3\mathbf{k}\, V_i^*(\mathbf{k}) V_j(\mathbf{k}) k^2 e^{i\mathbf{k}\cdot(\mathbf{r}_i - \mathbf{r}_j)} \delta(\omega_0 + \mathbf{k}\cdot\mathbf{v}). \end{aligned} \tag{10}$$

The error made at small impact parameters will be shown below to be negligible.

1. Randomly oriented clusters

Assuming randomly oriented clusters we may average $\mathbf{r}_i - \mathbf{r}_j$ in Eq. (10) over the unit sphere. Assuming a random target we may also average $\mathbf{v}$ over the unit sphere. The combined result is

$$\delta S = \frac{4\pi^4}{mv^2} \sum_{i \neq j} \int_{k>k_{\min}} 4\pi k^2 \, dk \, V_i^*(k) V_j(k) k \frac{\sin k r_{ij}}{k r_{ij}}, \tag{11}$$

where $k=|\mathbf{k}|$, $k_{\min}=\omega_0/v$, and $r_{ij}=|\mathbf{r}_i-\mathbf{r}_j|$.

If the contribution from incoherent stopping, $S_0 = \int d^2\mathbf{p}\, T_0$ were treated in the same manner, the result would differ from Eq. (11) by the absence of the factor $\sin k r_{ij}/k r_{ij}$ and the replacement of the double sum by a single sum with $i=j$. In this simplified form, S_0 would diverge logarithmically at large k. In the quantitative theory of incoherent stopping that divergence is avoided by replacement of the dipole approximation at small impact parameters by the law of free-Coulomb scattering [29,28]. This produces an effective upper limit of the order of $k_{\max} \simeq mv^2/Z_1 e^2$.

Equation (11) shows a very different behavior at large values of k: The logarithmic divergence is removed by the additional factor of $1/k$, and the oscillatory factor $\sin k r_{ij}$ generates an effective upper limit $k_{\max,\mathrm{eff}} \sim 1/r_{ij}$. The combined effect of these two features drastically reduces the contribution to the integral from large values of k or small values of p and therefore justifies the rather rough approximation applied to small impact parameters in the above integration.

2. Aligned clusters

Orientational effects are most pronounced for linear molecules. We consider diatomics only. For a diatomic molecule aligned with the beam direction, Eq. (8) reduces to

$$T(p) = T_1(p)\left(1 + \cos\frac{\omega_0 r_{12}}{v}\right), \tag{12}$$

where $T(p)$ is the energy loss per cluster atom and $T_1(p)$ the energy loss for an atomic ion. It follows that the correction factor for coherent stopping is independent of the impact parameter in this particular geometry. Therefore, a corresponding relation applies to the stopping cross section for a single resonance,

$$S = S_1\left(1 + \cos\frac{\omega_0 r_{12}}{v}\right). \tag{13}$$

This relation was established in Ref. [30].

B. Bethe theory

The dielectric theory of stopping [24,22] incorporates a proper (quantal) treatment of close collisions which does not invoke the dipole approximation. We sketch the equivalent of the above derivation within that framework in order to further demonstrate that neglecting the error made in the limit of close collisions is justified. For the coherence correction to the stopping power of an electron gas with a density n for a randomly oriented cluster we find

$$\delta\left(\frac{dE}{dx}\right) = \frac{4\pi^3}{e^2 v^2} \sum_{i \neq j} \int_0^\infty dk\, k^3 \times \int_{-kv}^{kv} d\omega\, i\omega \left(\frac{1}{\epsilon(k,\omega)} - 1\right) V_i^*(\mathbf{k}) V_j(\mathbf{k}) \frac{\sin k r_{ij}}{k r_{ij}}. \tag{14}$$

We have evaluated Eq. (14) for the dielectric function of an electron gas at rest [22],

$$\epsilon(k,\omega) = 1 + \frac{\omega_P^2}{\omega_k^2 - (\omega + i\gamma)^2} \tag{15}$$

with $\omega_k = \hbar k^2/2m$ and $\omega_P = \sqrt{4\pi n e^2/m}$ the plasma frequency and γ an infinitesimal damping constant. This results in Eq. (11) with the integration limits changed to

$$k_{\min} = \frac{\omega_P}{v}; \quad k_{\max} = \frac{2mv}{\hbar} \tag{16}$$

for $mv^2 \hbar \omega_P$. Although we deal with different physical systems, it is justified to consider the plasma frequency ω_P of the electron gas as an equivalent of the resonant frequency ω_0 of an individual oscillator. With this, the main difference between the two expressions lies in the upper integration limits $k_{\max}$ which reflect the classical and the perturbation limit, respectively [20]. At the same time the difference in the treatment of close collisions is confirmed to be immaterial.

C. Exponential screening

We now introduce an exponentially screened Coulomb interaction [31,30,28],

$$V_i(r) = \frac{-Z_i e^2}{r}\left[\beta_i + (1-\beta_i) e^{-\kappa_i r}\right], \tag{17}$$

or

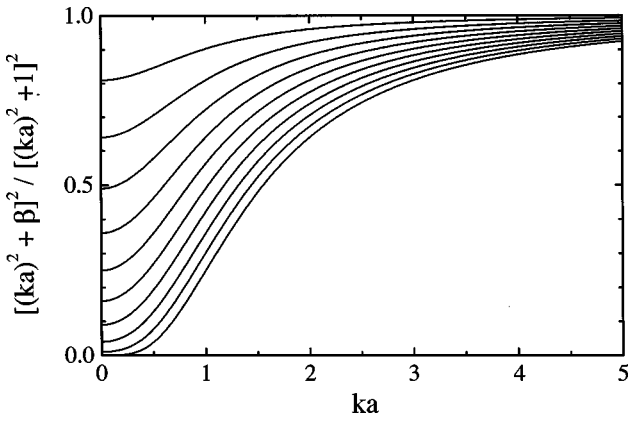

FIG. 2. Charge-state-dependent factor in the integrand determining coherence correction to stopping cross section, Eq. (20). Homonuclear cluster and same charge fraction $\beta_j \equiv \beta = q_1/Z_1$ assumed for all atoms. Curves for β running from 0 to 1 in steps of 0.1 (bottom to top).

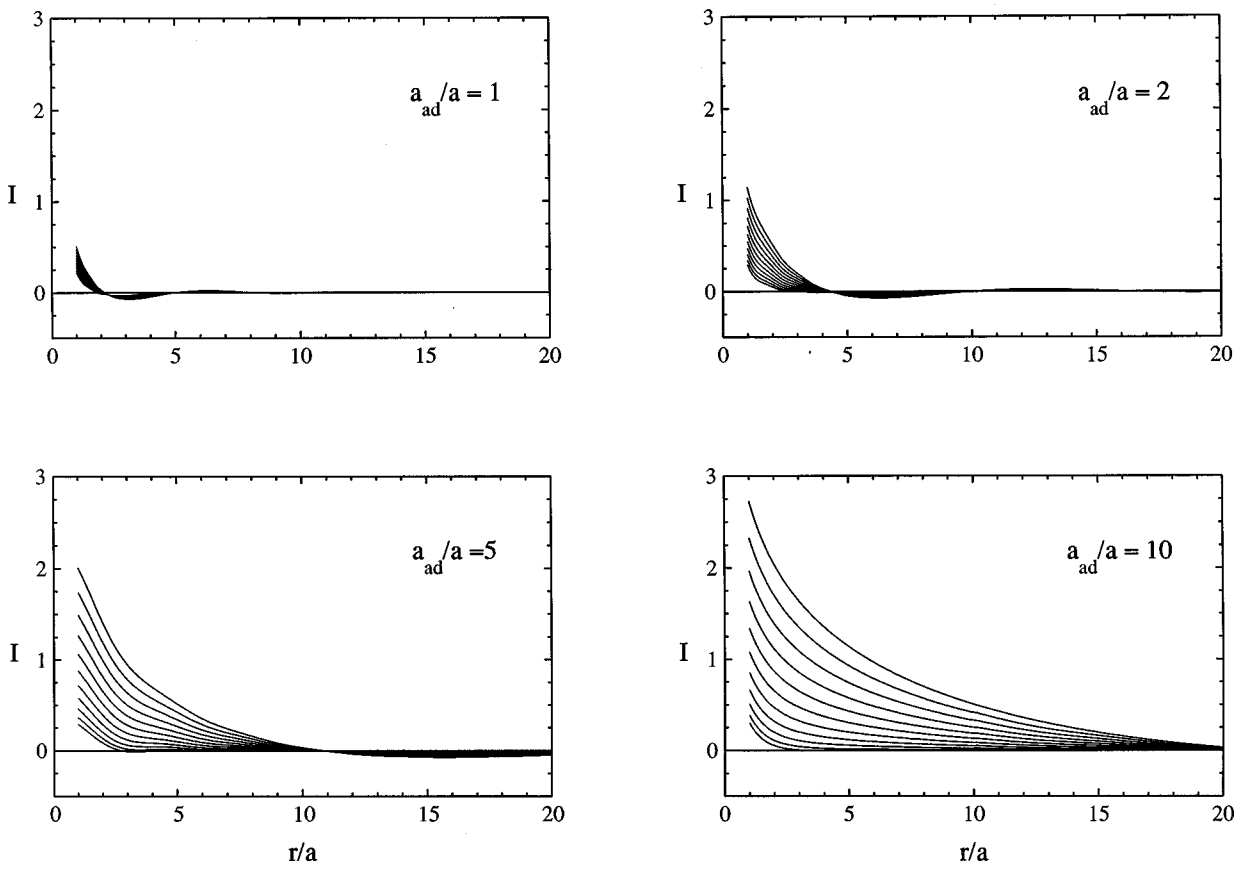

FIG. 3. The integral $I(r,\beta)$ defined by Eq. (20) for pairwise identical charge fractions $\beta=q/Z$. The eleven curves on each graph represent values of β going from 0 to 1 in steps of 0.1 (bottom to top). The four plots reflect four values of the ratio $v/\omega_0 a$ between the adiabatic radius and the screening radius.

$$V_i(\mathbf{k})=\frac{Z_i e^2}{2\pi^2}\frac{k^2+\beta_i\kappa_i^2}{k^2(k^2+\kappa_i^2)}, \tag{18}$$

where $\beta_i=q_i/Z_i$ is the charge fraction on the ith ion and $\kappa_i^{-1}=a_i$ the screening radius. With this, Eqs. (11) and (14) reduce to

$$\delta S=\frac{4\pi e^4}{mv^2}\sum_{i\neq j} Z_i Z_j I_{ij}(r_{ij},\beta_i,\beta_j) \tag{19}$$

with

$$I_{ij}(r_{ij},\beta_i,\beta_j)=\int_{k_{\min}}^{k_{\max}}\frac{dk}{k}\frac{(k^2+\beta_i\kappa_i^2)(k^2+\beta_j\kappa_j^2)}{(k^2+\kappa_i^2)(k^2+\kappa_j^2)}\frac{\sin kr_{ij}}{kr_{ij}}. \tag{20}$$

Equation (20) reduces to a well-known result [24]

$$I_{ij}(r_{ij},\beta_i=\beta_j=1)=g(k_{\min}r_{ij})-g(k_{\max}r_{ij});$$

$$g(\xi)=\frac{\sin\xi}{\xi}-Ci(\xi) \tag{21}$$

in the limit of complete stripping, $\beta_i=1$. Here $Ci(\xi)$ is a cosine integral [32]. The same limit could have been found by letting the screening radius go to infinity, i.e., $\kappa_i=0$. It is readily seen that the accurate choice of the upper limit $k_{\max}$ in Eq. (21) is immaterial as long as $k_{\max}r_{ij}\gg 1$. Note that

$$g(\xi)\sim\frac{\cos\xi}{\xi^2}\quad\text{for}\quad\xi\gg 1. \tag{22}$$

The integrand in Eq. (20) differs in two aspects from the one for an isolated point charge. (1) The factor $\sin kr_{ij}/kr_{ij}$ produces an effective upper limit of integration $\simeq r_{ij}^{-1}$, and (2) the factor containing β_i and κ_i reduces the integrand at small k (Fig. 2). Specifically, for small values of β, i.e., for near-neutral clusters, Eq. (20) yields an effective lower limit of integration $k_{\min}\simeq\kappa_i$.

Figures 3 and 4 show values of the integral

$$I(r_{ij}=r,\beta_i=\beta_j=\beta) \tag{23}$$

for pairwise identical charge states as a function of r_{ij}/a (Fig. 3) and charge fraction β (Fig. 4). Integrations have been carried out for $k=k_{\min}\cdots\infty$. This implies a slight overestimate of I for $mv^3/Z_1e^2\omega_0\lesssim 2$.

The sequence of graphs demonstrates that coherence corrections (1) decrease with increasing internuclear distance, (2) increase with increasing projectile velocity, and (3) are approximately proportional to the square of the charge frac-

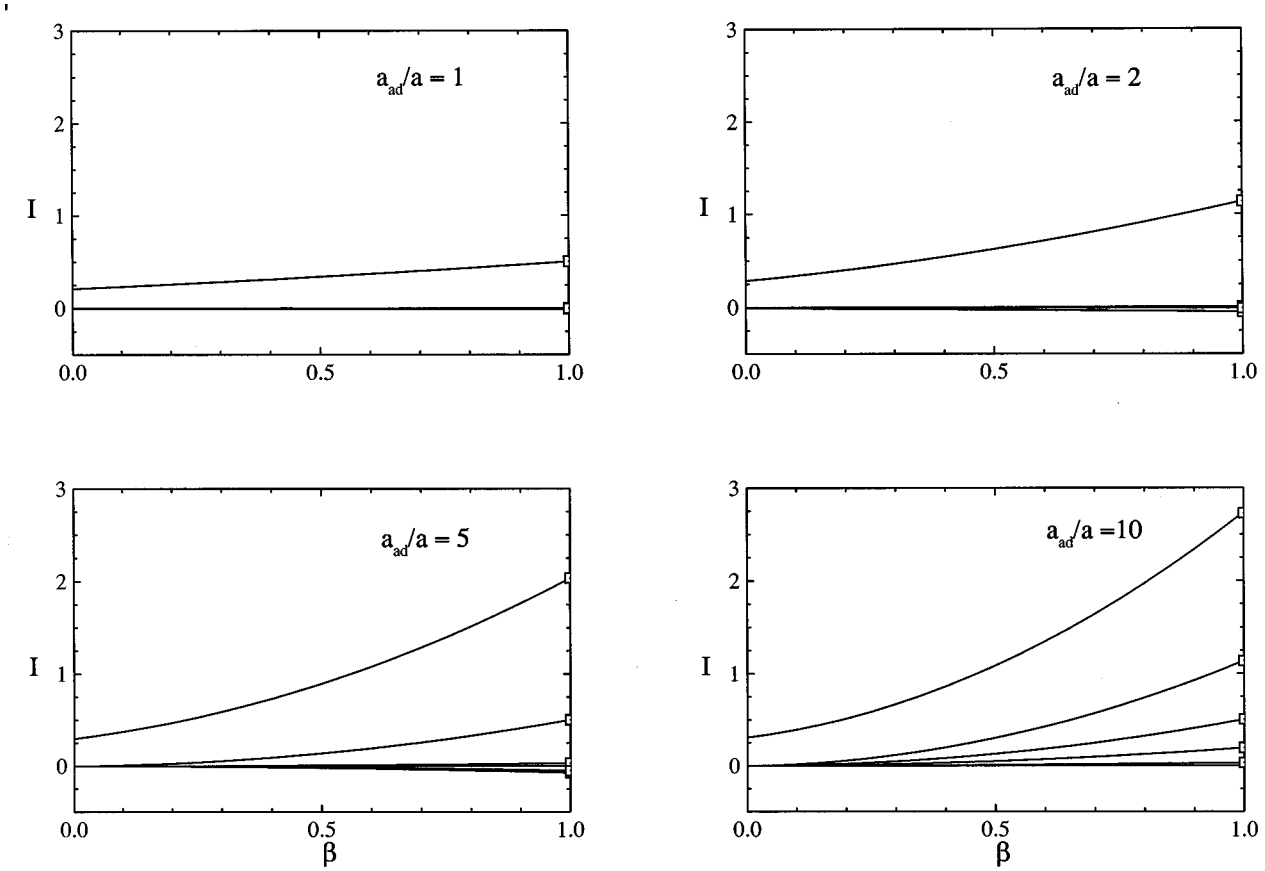

FIG. 4. Same as Fig. 3 plotted as a function of charge fraction. The five curves on each graph represent values of $r/a=1,5,10,15,20$ from top to bottom. The four plots reflect four values of the ratio between the adiabatic radius and the screening radius. Squares indicate values evaluated directly from Eq. (21).

tion $\beta=q_1/Z_1$. These properties are all consistent with the fact that I reflects long-range interactions.

D. Spectrum of target resonances

For a target with one heavily dominating resonance, the stopping ratio for a randomly oriented homonuclear diatomic molecule reduces to

$$R=1+\frac{I}{L}, \tag{24}$$

where indices in $I=I_{ij}$ have been dropped, and where $L=L_i$ is the stopping number for an individual atomic ion,

$$S=\frac{4\pi Z_1^2 e^4}{mv^2}L. \tag{25}$$

R as given by Eq. (24) depends only on the parameter $\omega_0 r/v$ where r is the internuclear distance. All other parameters, in particular, the atomic number of the projectile, drop out. It is tempting to assign a high degree of generality to Eq. (24). This, however, is by no means justified.

Staying with a randomly oriented diatomic homonuclear molecule but allowing for a realistic spectrum of target resonances we obtain

$$R=1+\frac{\Sigma_n I_n}{\Sigma_n L_n}, \tag{26}$$

instead of Eq. (24), where n denotes individual target resonances ω_n.

The numerator in Eq. (26) hinges on low-lying resonances (which are associated with a high adiabatic radius) at all projectile speeds. While the denominator draws its leading contributions from the lowest resonances at low speed, higher excitation channels get increasingly important with increasing speed. For targets with moderate and high atomic number the denominator eventually gets dominated by higher resonances. Thus, after an initial increase due to increasing adiabatic radius [10], R must decrease with increasing projectile velocity. This finding is in sharp contrast with the estimates presented in Ref. [17] based on a single resonance.

Incorporating the spectrum of target resonances is straightforward within the Bohr theory, where target subshells are weighted by tabulated oscillator strengths [33]. The same is true when the harmonic-oscillator model of electronic stopping [34] is applied to clusters [13]. In the dielectric theory, the local-density approximation [35] is an appropriate tool. This is very common in the theory of light-ion stopping, but in the theory of coherent stopping this step has

most often been omitted, with the notable exception of Ref. [19].

E. Z_1^3 correction

The Z_1^3 (or Barkas) correction arises from the response of the stopping medium to the penetrating ion. It is significant at velocities low enough for target electrons to relax so much as to influence excitation cross sections. For a given resonance and an unscreened ion, this correction is smaller by a factor $\propto Z_1 e^2 \omega_0 / m v^3$ than the leading term in the stopping cross section [36,37]. For a positively charged projectile the correction is positive.

The Z_1^3 correction has more or less tacitly been ignored in studies of coherent stopping. This could have been justified by noticing that coherent stopping prevails at projectile speeds ($v > \omega_0 r$) while a noticeable Z_1^3 correction occurs for, say, $Z_1 e^2 \omega_0 / m v^3 > 0.1$. For a small internuclear distance $r \simeq 1$ Å, both conditions can be fulfilled if

$$Z_1 > \left(\frac{\hbar \omega_0}{e^2 / a_0} \right)^2, \tag{27}$$

where a_0 is the Bohr radius. This is uninteresting for light ions but becomes relevant for higher Z_1.

Estimates of the Z_1^3 correction for screened heavy atomic ions are on their way [38]. At this point we only wish to demonstrate that inclusion of the Z_1^3 effect *decreases* the significance of coherent stopping.

Consider unscreened ions first. Since the Z_1^3 correction is positive, all terms in the denominator of Eq. (26) will increase. Because of the $Z_1 e^2 \omega_n / m v^3$ dependence on the respective resonance frequencies ω_n, the change due to the Z_1^3 correction is most pronounced in the inner-shell terms. Also terms in the numerator will increase, but this is noticeable only for those where $\omega_n < v/r$, i.e., for outer shells. Thus, the increase in the denominator will in general be more pronounced than in the numerator.

Inclusion of projectile screening into the above argument primarily reduces the contribution of the lowest target resonances in Eq. (26) but does not affect the sign of the correction. In conclusion, even though the Z_1^3 correction may be more pronounced for a screened than for an unscreened atomic ion, its consideration in cluster stopping will reduce coherent stopping.

F. Examples

The examples discussed below are based upon the following package of assumptions.

(1) Cluster are homogeneous with an equilibrium charge per atom $q_1 e = \beta_1 Z_1 e$.

(2) The equilibrium charge is given by Thomas-Fermi type expression

$$\beta_1 = 1 - e^{-v / Z_1^{2/3} v_0}, \tag{28}$$

(3) Only electronic stopping by target excitation or ionization is considered.

(4) The screening model is defined by Eq. (17) and the screening radius is given by

$$a = a_{TF}(1 - \beta_1) \tag{29}$$

with $a_{TF} = 0.8853 a_0 Z_1^{-1/3}$ according to Ref. [28].

(5) Stopping numbers L for incoherent stopping and corrections I for coherent stopping are evaluated for every target subshell, cf. Sec. III D.

(6) Incoherent stopping is evaluated for modified Bohr and modified Bethe stopping.

(7) Interference functions I are evaluated either with $k_{\max} = \infty$ or with the quantal upper limit $k_{\max} = 2mv/\hbar$. The difference between these cases was invisible in all quoted examples. Therefore only the results for $k_{\max} = \infty$ (labeled ''Bohr'') are shown.

Figure 5 and Table I show the results for hydrogen on carbon for reference. Calculations have been performed for both screened and unscreened ions. The Bethe theory is valid for $v \gtrsim 2v_0$, i.e., over most of the velocity range covered in the graph. The total stopping cross section is somewhat lower than what would follow from Bohr's expression, mainly due to different contributions from the carbon K shell. As expected, the K shell does not contribute visibly to coherent stopping. L-shell electrons show enhanced stopping in qualitative agreement with previous estimates [10]. Representative enhancement factors are given in Table I. If stopping powers were estimated on the basis of the Bohr theory, predicted relative enhancements would be slightly smaller. Note the insensitivity of both L and I to projectile screening. This is consistent with the finding from Ref. [28] that stopping is insensitive to the charge state for $Z_1 \ll Z_2$. This, in turn, justifies the neglect of screening in existing theoretical treatments of coherent stopping for hydrogen clusters.

Figure 6 shows similar results for carbon on carbon. Here the Bohr theory is superior to the Bethe description over the entire velocity range covered by the graph. The Bethe prediction has been included for reference only. Interference functions for unscreened ions are identical with those for hydrogen. The same is true for the stopping number for unscreened ions in the Bethe theory. While all contributions are reduced by screening, the reduction is greatest in the interference function and smallest in the incoherent stopping number for the Bethe case. Note in particular that the interference function drops far below the stopping number in the velocity range where measurements have been reported, $v \lesssim 5v_0$. Moreover, in sharp contrast to the above results for hydrogen (Fig. 5), these results are sensitive to projectile screening.

Figure 7 shows stopping ratios calculated with and without screening. The two curves approach each other at high velocities where screening becomes negligible. The two trends discussed in Sec. III D are seen to produce a maximum enhancement of $\simeq 1.35$ and $\simeq 1.40$ near $v = 5v_0$ for screened and unscreened interaction, respectively. In the case of screening, that maximum is rather flat toward the high-velocity side but drops rapidly with decreasing speed.

For larger clusters one deals with a distribution of internuclear distances. In view of the rapid decrease of the inter-

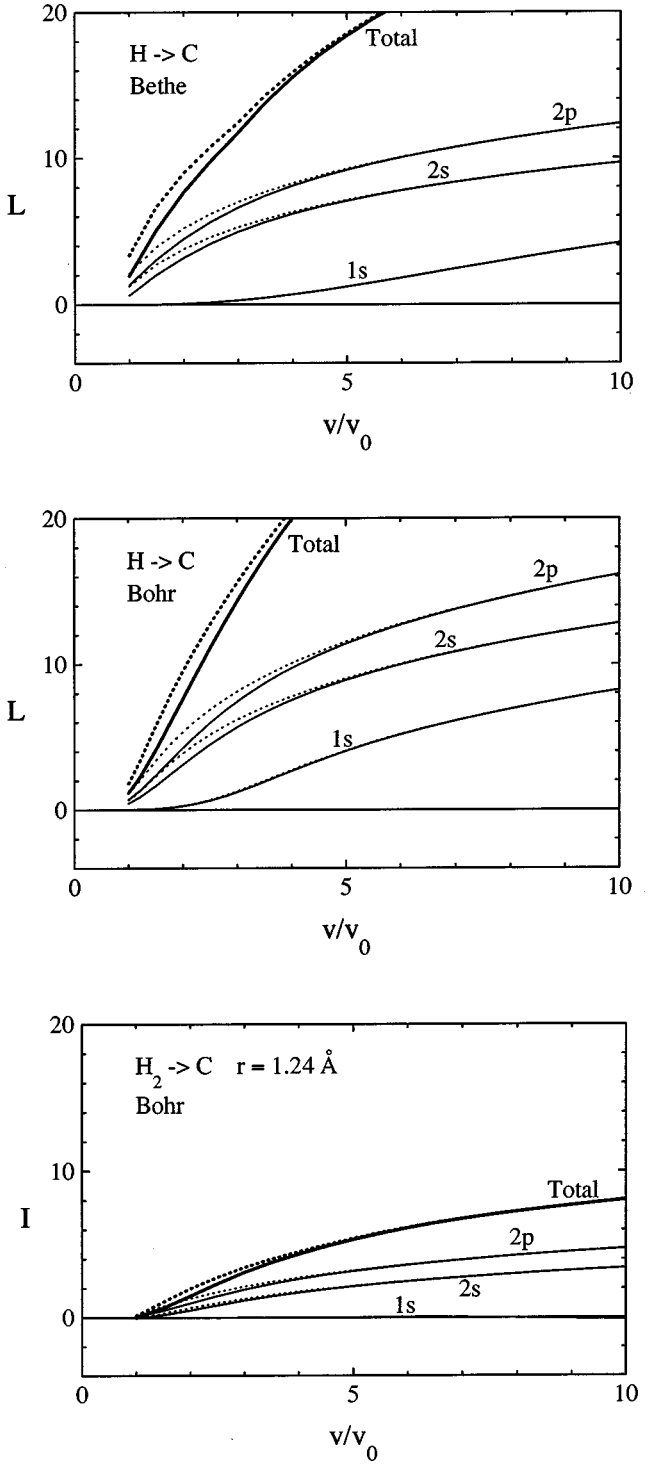

FIG. 5. Calculated stopping number (top and middle) and interference function (bottom) for hydrogen on carbon; constant internuclear distance r; contributions from target subshells and total; solid lines: screening included; dotted lines: screening excluded; modified Bethe theory (top) and modified Bohr theory (middle); bottom graph valid for both theories.

ference function with the internuclear distance (Fig. 3), coherent stopping is mostly due to nearest neighbors. Therefore, the stopping ratio for a large cluster [39,40] is expected to be $R<1+zI/2L$, where z is the coordination number and the inequality arises from surface atoms. This is an order of magnitude less than the enhancements reported in Ref. [17].

TABLE I. Interference function I, stopping number L for incoherent stopping, and stopping ratio $R=1+I/L$ at three velocities for hydrogen dimer on carbon; constant internuclear distance $r=1.24$ Å; Bethe and Bohr theory including screening.

	I				L_{Bohr}	L_{Bethe}	R_{Bohr}	R_{Bethe}
v/v_0	$1s$	$2s$	$2p$	Total				
2	0.0038	0.50	0.98	1.48	7.62	7.64	1.19	1.19
4	−0.019	1.72	2.64	4.34	19.9	15.5	1.22	1.28
10	−0.11	3.41	4.74	8.04	37.2	26.9	1.22	1.30

IV. OTHER MOLECULAR EFFECTS ON STOPPING

Although target excitation is the dominating stopping mechanism for swift ions, this dominance is not as pronounced for heavy ions as it is for $Z_1=1$. Alternative stopping mechanisms such as projectile excitation or ionization and charge exchange contribute over limited velocity ranges. The present section serves to identify ways in which such effects could contribute to coherent stopping. We shall try to determine the direction of such effects and to get an indication of their significance, but the discussion will be mainly qualitative. The main goal is to demonstrate that with one exception, these effects cannot compete with the coherence effects treated in Sec. III.

A. Projectile excitation or ionization

Projectile excitation and ionization contribute significantly to stopping when the number of electrons carried by the projectile is comparable to or greater than that on the target, i.e., in the velocity range of heavy screening where stopping by target excitation and ionization is mostly due to outer electrons. The process can become dominant when the number of weakly bound projectile electrons exceeds the number of weakly bound target electrons, i.e., for near-neutral ions with $Z_1>Z_2$ at velocities $v\ll Z_1^{2/3}v_0$. Here, Z_2 denotes the atomic number of the target material.

In the present context the question is whether molecular effects are to be expected in projectile excitation. A hint at an answer may be found by switching to a reference frame moving along with the projectile, where the process reduces to the equivalent of target excitation in the laboratory system. Note, though, that the ''target'' need not be completely neutral nor in the ground state. Viewed from this reference frame, a possible molecular effect in projectile excitation/ionization becomes the equivalent of deviations from Bragg's rule of stopping-power additivity for target excitation.

Deviations from Bragg's rule are commonly very small, of the order of a few percent or less. If the same applies to the moving reference frame, such deviations are of only marginal interest in the analysis of cluster stopping.

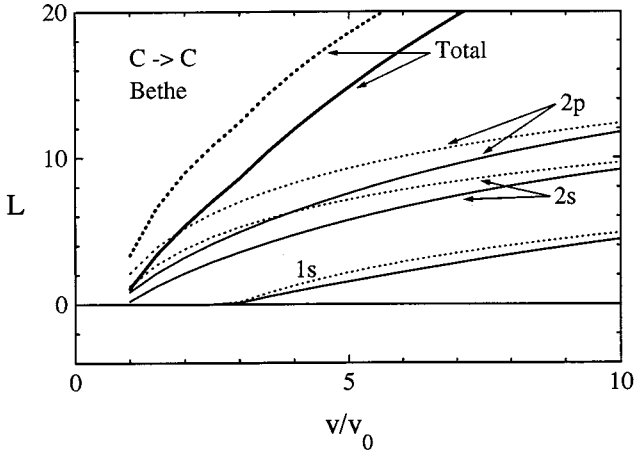

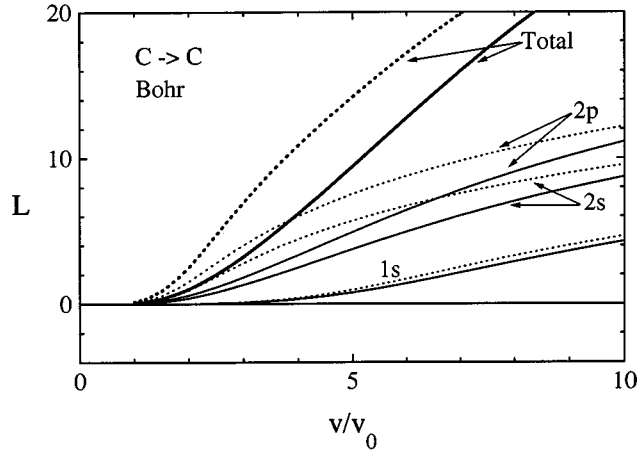

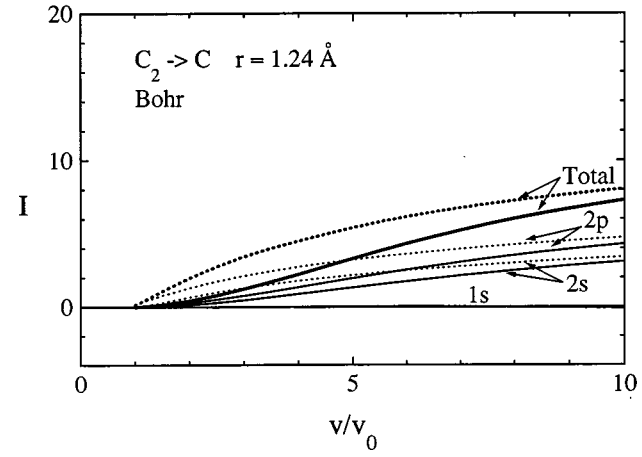

FIG. 6. Same as Fig. 5 for carbon on carbon.

Deviations from Bragg's additivity rule originate in differences in the states of valence electrons between molecules and independent atoms. Similar differences could be expected if molecules or clusters moving through a solid were literally bound. While this is possible it is barely the rule.

We conclude that even though projectile excitation and ionization may constitute a significant and even dominant contribution to the stopping power for a heavy ion, a possible molecular effect is generally small. Therefore, the relative

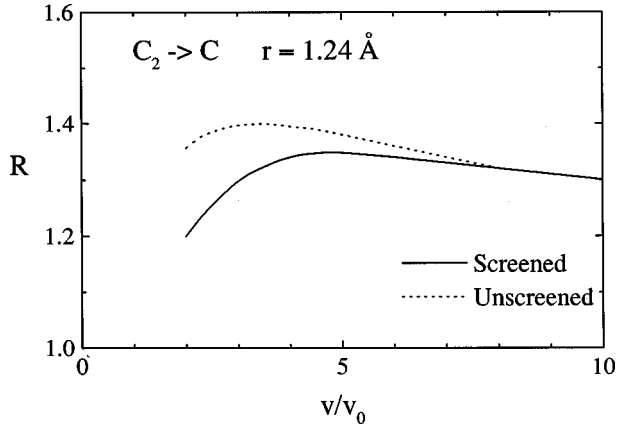

FIG. 7. Stopping ratio for C_2 on C evaluated from data shown in Fig. 6.

significance of coherent stopping by target excitation or ionization will get diminished by an increasing contribution to stopping by projectile excitation or ionization.

B. Energy loss by charge exchange

Energy loss in charge-exchange events constitutes an interesting aspect of heavy-ion stopping [41]. It affects primarily the statistics (straggling). Effects in the mean energy loss become noticeable mainly at low velocities when the cross section for stopping by Coulomb excitation becomes small and reaction channels involving charge exchange become more efficient [42]. Therefore, despite experimental evidence in favor of molecular effects in charge exchange (cf. below) we do not consider energy loss by charge exchange to contribute to molecular effects in stopping power in the velocity range considered in the present paper.

C. Charge-state effects

The stopping power for a given projectile depends on the charge state. Therefore, any molecular effect in the charge state must potentially affect the stopping power. It was shown in Ref. [28] that the sensitivity of the stopping power to the ion charge is governed by the parameter

$$s=\left(\frac{Z_1 e^2/a_0}{\hbar\omega_0}\right)^{2/3}. \tag{30}$$

Specifically, Fig. 7 in that work indicates very little sensitivity for $s\ll 1$, while for $s\gg 1$ a q_1^2 (or β_1^2) dependence is approached.

To the extent that the target may be characterized by a single resonance frequency equivalent with the mean excitation energy, Eq. (30) reduces to [28]

$$s\simeq 2\left(\frac{Z_1}{Z_2}\right)^{2/3}. \tag{31}$$

Thus, molecular effects due to varying charge states are predicted to be insignificant in the limit $Z_1\ll Z_2$.

One may distinguish between effects on the equilibrium charge state and on charge equilibration. Solid experimental

or theoretical evidence on the former does not appear to be available but it appears feasible that electron-capture processes are affected by the proximity of other moving nuclei. In particular, electrons lost by a moving nucleus may be captured by another nucleus in the neighborhood. Moreover, the combined attractive potential of the ion cores of a cluster could provide increased binding in comparison to an isolated atomic ion.

The situation is more clearcut with regard to charge equilibration. After all, clusters emerge from an ion source in low charge states, mostly singly or doubly charged regardless of size. Hence, while an atomic ion can have any charge from 0 to Z_1, the mean incident charge state per cluster atom is typically $1/n$ or perhaps $2/n$ and rarely more.[1] Thus, already at moderately high projectile speeds ($v \simeq Z_1^{2/3} v_0$) the charge state per cluster atom is bound to increase with traveled path length. This implies low initial stopping powers and a gradual increase toward equilibrium.

Little theoretical guidance seems available on charge equilibration of cluster beams. A united-atom picture proposed in Ref. [9] (and reproduced in Ref. [16]) may contain essential features but is unquestionably oversimplified. Some evidence is, however, available from experiments. Maor *et al.* [44] reported mean charges of nitrogen atomic and molecular ions as a function of penetrated-foil thickness at 2.1 MeV/atom. Target thicknesses range from somewhat below 10 nm to ~80 nm. An apparent equilibrium charge is found for molecular ions that is slightly smaller (≃4%) than for atomic bombardment. Much more pronounced is the difference in equilibration distance which is ≃30 nm for the molecule as compared to ≃10 nm for atomic ions of the same species at the same speed.

Brunelle *et al.* [45] report mean charges of carbon clusters ($n=3-10$) as a function of penetrated-foil thickness at energy 1–4 MeV/atom. Mean charge states are found to increase in all cases when the foil thickness increases from 2.2 to 40 μg/cm^2. Mean charges approach the atomic equilibrium charge at large path lengths, but the equilibration distance is found to increase with cluster size.

This leads to the following picture.

(1) In the velocity range of partial stripping in equilibrium, $v \simeq Z_1^{2/3} v_0$, incident clusters have typically low charges that are bound to increase with path length.

(2) For certain systems the equilibration depth depends on the state of aggregation. The systematics are unknown, but experimental evidence is available for increasing equilibration depth with increasing cluster size.

(3) For $Z_1 \gtrsim Z_2$ the stopping cross section is sensitive to the charge state.

(4) Therefore, the stopping power per cluster atom remains below the equilibrium value for a substantially longer path length than for atomic bombardment.

Experimentally, this will show up as a coherence effect. Note, however, that here we deal with negative enhancement. An upper bound on the magnitude of this effect is the difference in stopping power between a completely stripped and a neutral atom. According to Fig. 7 in Ref. [28], this difference may be very large, dependent on the magnitude of the parameter s, Eq. (30).

D. Clearing-the-way effect

We note the clearing-the-way effect mainly as a curiosity, because (a) it originates in close collisions, (b) it gives rise to negative enhancement, and (c) it is strongly nonlinear.

Its effect on cluster stopping has been discussed in connection with nuclear stopping [46] and was found in computer simulations [47,48]. When the projectile mass exceeds that of the target particle, target particles recoiling from a leading cluster atom may not be available for collisions with trailing cluster atoms. This feature requires cross sections large enough so that a noticeable fraction of the target particles is knocked on.

These considerations should remain valid also for electronic collisions,[2] especially for heavy projectiles where this kind of process is invoked to explain the formation of visible tracks via Coulomb explosion. It has also been argued that the effect could be responsible for an observed sublinear behavior of electron emission yields [49].

We stress that this effect, being nonlinear, is not included in the common linear theory of wake effects, based on the dielectric theory of the electron gas [22] and valid for weakly interacting low-Z_1 ions. That picture predicts a *pileup* of weakly scattered electrons in the region *behind* the leading projectile atom. The key point of the present picture is a substantial *depletion.*

V. DISCUSSION OF EXPERIMENTS

A. Multiple scattering and Coulomb explosion

For a valid comparison with experimental results the variation of the internuclear distance r with penetrated foil thickness (''dwell time'') needs to be taken into account. This variation is caused by Coulomb explosion and multiple scattering and hence depends on the charge state. Initially, Coulomb explosion, being a one-way process, tends to dominate while multiple scattering takes over at larger path lengths when r has increased to a value where the Coulomb force is negligible. However, multiple scattering may be dominating for near-neutral projectiles.

When estimating Coulomb explosion we determine $r = r(t)$ from the classical equation of motion and set the ion charge equal to the equilibrium charge state.

B. Randomly oriented molecules

We focus on the C_n-C system ($n=1,\ldots,6$) which has been studied most extensively [14–16]. Measurements were

[1]The statement does not apply to double-foil experiments of the type reported in Ref. [43].

[2]The authors are grateful to L. C. Feldman for making us aware of this possibility.

performed at energies per atom ranging from 0.33 to 4.2 MeV, i.e., for v/v_0 ranging from 1.0 to 3.7 where screening is significant (Fig. 1). Target thicknesses are comparable and range from ~200 to 2000 Å.

A common feature of all experimental data is that deviations from incoherent stopping are astonishingly small, so small that a detailed explanation of the observed deviations from incoherent stopping as well as differences between different experimental data is near the borderline of the scope of the present paper.

Figure 7 indicates that stopping ratios for target excitation or ionization at an internuclear distance of $r=1.24$ Å increase with increasing velocity in the energy range covered by experiments. This feature is consistent with the Orsay measurements [14] ($2<v/v_0<3.7$ for $n=2$ to 8). The Erlangen data [15] ($1<v/v_0<2.6$ for $n=2$ to 5) do not show a significant variation with energy. This is consistent with the fact that the predicted effect is smaller at those low velocities (Fig. 7).[3] Moreover, these measurements were performed on somewhat thicker foils, with the consequence of a minor decrease in coherent stopping due to multiple scattering and Coulomb explosion. The Rehovoth measurements [16] ($3.1<v/v_0<3.6$) do not show a significant variation with beam energy over the small range covered.

With regard to the sign of the enhancement effect, we note that the Orsay measurements show negative enhancement at $v/v_0=2$, which is in clear contradiction with Fig. 7. The same discrepancy is found with the Rehovoth measurements. The Erlangen measurements, on the other hand, yield stopping ratios greater than 1, albeit with large error bars.

With regard to the absolute magnitude we first note that the predicted enhancement amounts to at most $R=1.3$ in the pertinent velocity range for a pair separated by $r=1.24$ Å. However, according to standard multiple scattering theory [50,51], the lateral spread of an individual carbon ion traveling through a foil 250 Å thick is about 2 Å at 1 MeV and 0.5 Å at 4 MeV. This implies that even for the Orsay measurements—which employed the thinnest foils—internuclear distances at exit have increased significantly. At the lowest velocities this increase is beyond the range where significant coherent stopping can be expected. The same statement applies to all data from the Erlangen group.

Despite large apparent scatter, the Orsay data show a tendency for increasing stopping ratios with n increasing from 2 to 4 and a distinctly smaller value for $n=5$. This could be explained in terms of the structure of these clusters with an increasing number of neighbors for $n=1,\ldots,4$ and a more open structure when n goes beyond 4, representing a tetrahedron.

What remains to be explained is the fact that observed positive enhancements in the Orsay measurements at the highest velocities are smaller than estimated theoretically, and that the low-velocity measurements at Orsay as well as the measurements at Rehovoth indicate negative enhancements instead of a minor positive or vanishing enhancement. Both features are asserted to be due to charge equilibration. The range of thicknesses here is the same as in the measurements [45] discussed in Sec. IV C. For the C-C system, the factor s governing the effect of the charge state on stopping power is $s=3.57$ for the carbon L shell according to Eq. (30). This implies an increase in stopping power by ~40% from charge fraction 0–0.5 in the velocity range in question. For small clusters the initial charge fraction is significantly greater than 0. For large clusters the final charge state is significantly smaller than 0.5. Hence, the variation in fractional charge will be significantly less than 40% for all clusters. This effect is less significant for the Erlangen measurements because of the larger foil thicknesses employed there. Moreover, projectile excitation and ionization provide a major contribution at the velocities studied there.

Finally we note that reported measurements on C_{60} were done at $v/v_0=0.8$, i.e., at a velocity where the present scheme is not expected to even qualitatively apply.

In conclusion we find that many qualitative features in measurements reported on the C_n-C system are consistent with our predictions, in particular, the absence of any pronounced enhancement effects. More quantitative predictions would require detailed structures and dimensions of incident clusters, a more detailed knowledge of charge equilibration, and, last but not least, a more accurate and comprehensive base of experimental data for comparison.

C. Aligned molecules

We include a brief discussion of experimental data on aligned molecules, mainly because the only existing set of data has received considerable attention without having been really explained.

Energy-loss measurements were performed on nitrogen and oxygen diatomic ions in an experimental geometry where only molecules were recorded that emerged from the stopping foil oriented in a narrow cone around the beam direction [12,52]. Reported enhancement factors lie consistently below 1 and increase monotonically with increasing foil thickness from some value R_0 toward 1. R_0 appears to increase with projectile speed from slightly below to slightly above 0.90 in the velocity range covered, $1.20<v/v_0<2.28$, although this variation is barely outside the error bars. Thus, the effect is small in terms of what we try to address in this paper.

Initial attempts at an explanation in terms of wake forces on moving point charges [12,52] failed to produce the observed trends. Other estimates were based on an electron wind model [52,53], i.e., scattering on free, noninteracting target electrons. Enhanced screening for penetrating molecules as compared to penetrating atoms was postulated in order to produce negative enhancement ratios. A subsequent calculation from first principles [30] had a somewhat similar starting point as the one reported above, i.e., stopping by target excitation of a molecule made up by two screened

[3]An estimate for $1<v/v_0<2$ has not been included in Fig. 7 because of a significant expected Z_1^3 correction. However, as argued in Sec. III E, inclusion of such a correction would reduce incoherent stopping. This again is consistent with the experimental observation.

TABLE II. Stopping of N_2 molecules aligned with the beam. Columns representing energy/atom, projectile speed, factor $\cos\omega_0\tau$ in Eq. (13) with $\tau=r_{12}/v$, calculated equilibrium charge fraction, calculated stopping ratio (screened/unscreened) for atomic ion with mean equilibrium charge, ratio of stopping ratios for atomic ions in incident and mean equilibrium charge, and measured stopping ratio at lowest film thickness [12].

E/atom (MeV)	v/v_0	$\cos\omega_0 t$	$\beta_{\rm equ}$	$F_{\rm equ}$	$F_{\rm in}/F_{\rm equ}$	Expt
1.8	2.27	0.67	0.46	0.40	0.70	0.92
1.5	2.07	0.61	0.43	0.38	0.74	0.92
1.2	1.85	0.52	0.40	0.36	0.78	0.90
1.0	1.69	0.43	0.37	0.35	0.80	0.88
0.8	1.51	0.32	0.34	0.34	0.82	0.89
0.5	1.20	0.01	0.28	0.32	0.88	0.87

ions. The target was characterized as a free-electron gas, and the description was quantal.

If the observations are to be explained in terms of target excitation or ionization, the proper starting point is Eq. (13). Values of $\cos\omega_0\tau$ with $\tau=r_{12}/v$, calculated for an average value of $\hbar\omega_0=24.0$ eV characterizing excitation of the L shell and [54] $r_{12}=1.12$ Å are shown in Table II as a function of projectile speed. It is seen that $\cos\omega_0\tau$ is positive but approaches zero at the lowest projectile speed. Since r_{12} increases as a result of Coulomb explosion and multiple scattering, negative enhancement must be expected at least for the lowest projectile speed which happens to be the one where the largest negative enhancement was found experimentally.

Figure 8 shows a comparison with measured stopping ratios versus dwell time (equivalent with foil thickness) taking into account Coulomb explosion on the basis of equilibrium atomic charge states, Eq. (28), for the highest and lowest projectile speed where measurements were made. It is seen that in both cases, R turns negative over a certain range of target thicknesses, and that the magnitude of the effect is compatible with the experiments, although the (weak) dependence on projectile speed is opposite to that observed. The theoretical prediction based upon this picture has the character of a sharp resonance, very unlike the slow variation of the experimental points. Although that resonance will be broadened by a number of effects ignored here, such as a realistic excitation spectrum of the L shell and a spread in charge state, the present results do not encourage an interpretation of the experimental results solely in terms of interference in target excitation/ionization.

Table II also lists equilibrium charge fractions calculated from Eq. (28) for nitrogen atomic ions for energies pertaining to Ref. [12]. These values were used to evaluate stopping fractions $F_{\rm equ}$, i.e., ratios of the stopping cross section of an ion of charge q_1e and that of the bare ion (charge Z_1e). This conversion was performed on the basis of Fig. 7 of Ref. [28]. In view of the low velocity only the stopping due to carbon-L electrons was taken into account and characterized by a single resonant frequency $\hbar\omega_0=24.0$ eV [33]. In the same way the initial stopping fraction $F_{\rm in}$ was evaluated for the initial charge state $\beta_{\rm in}=0.5/Z_1$. This yields initial enhancement factors $F_{\rm in}/F_{\rm equ}$ increasing from 0.70 at 1.8 MeV/atom to 0.88 at 0.5 MeV/atom. Measured values given in Table II refer to the lowest foil thickness. Calculations seem compatible with the measurements to the extent that all experimental values lie closer to equilibrium than calculated ones, as they should in view of the nonvanishing foil thickness.

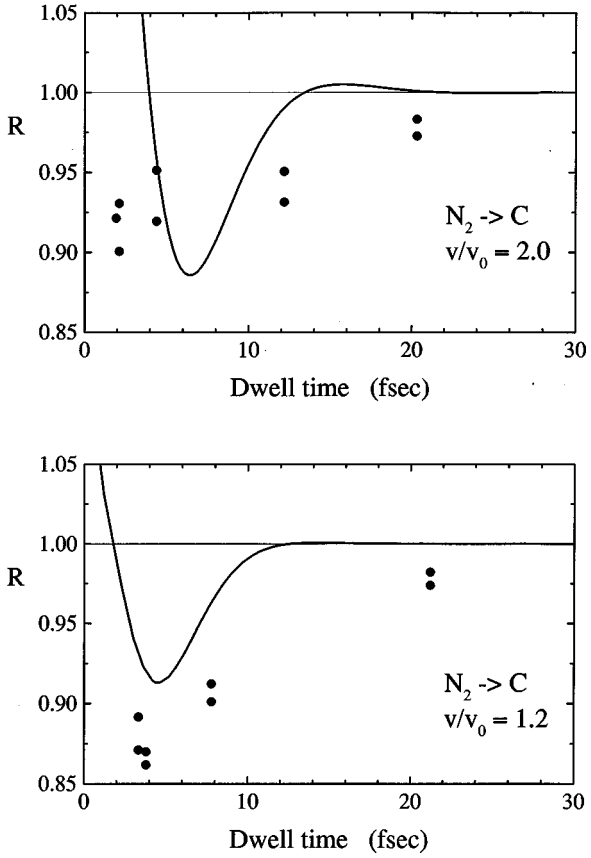

FIG. 8. Comparison of calculated with measured stopping ratio for N_2 molecules in carbon as a function of dwelltime (foil thickness). Measured values from Ref. [12]. Calculated values based upon Eq. (13) summed over shells, with an internuclear distance r_{12} varying across the trajectory due to Coulomb explosion, estimated on the basis of mean equilibrium charge for atomic nitrogen, Eq. (28). Upper and lower graphs refer to $v/v_0=2.0$ and 1.2, respectively.

However, calculations predict a more pronounced variation with projectile velocity than what has been found experimentally. Moreover, the measured variation with velocity, if significant at all, goes in the opposite direction.

We may note that these estimates do not invoke the internuclear distance r_{12} and hence do not warrant a treatment of Coulomb explosion.

With the stopping power per nitrogen atom exceeding 100 eV/Å a noticeable clearing-the-way effect of the type mentioned in Sec. IV D can be expected. Moreover, its energy dependence may be expected to be weak since measurements were performed at velocities around the stopping maximum. However, this effect does not generate rapid variations with thickness of the type found in Fig. 8.

VI. SUMMARY AND CONCLUSIONS

On the basis of both qualitative arguments and quantitative estimates we may conclude that deviations from the simple additivity rule of stopping powers for constituent atoms are not restricted to groups of penetrating point charges but are also expected for molecules and clusters made up by dressed ions. Our study addressed only swift ions ($v > v_0$).

Interference effects in target excitation/ionization by clusters heavier than hydrogen are qualitatively similar to what is known for hydrogen clusters but are reduced by projectile screening. This reduction increases with increasing screening, i.e., with decreasing velocity if there is charge equilibrium. Therefore, positive enhancements—which are typical at high projectile speed—are less dramatically reduced by screening than negative enhancements which, in contrast to hydrogen, are predicted to be barely visible for heavier clusters.

On a relative scale, predicted effects of coherent stopping due to target excitation and ionization never exceed predictions for hydrogen clusters. When the stopping power of an individual target subshell is considered, the significance of coherent stopping is found to increase monotonically with projectile speed. In the total stopping power, this increase is counteracted by an increasing (incoherent) contribution from inner shells. This gives rise to a maximum in the enhancement factor, an example of which is shown in Fig. 7. Neglecting these features has sometimes given rise to unrealistically large enhancements in stopping power [17].

The greatest enhancements in stopping power are evidently expected for targets that have no or only weakly bound inner-shell electrons, i.e., gaseous or solid hydrogen and fully ionized plasmas. In particular the latter case is interesting because of drastically reduced screening effects.

We note that there is no significant difference in absolute estimates of coherent stopping between the Bohr and the Bethe theory. Differences arise solely in relative enhancements due to different predictions for incoherent stopping between the two theories.

Effects competing with coherent target excitation/ionization have been discussed on qualitative grounds only. Projectile excitation and ionization, while contributing substantially to the stopping of slow clusters, are not expected to undergo a strong molecular effect, and the contribution of charge exchange to stopping is considered small altogether in the velocity range addressed for both atomic and molecular projectiles.

Effects in equilibrium charge and, especially, in charge equilibration, are found to be pronounced, in particular for large ratios Z_1/Z_2. While a detailed study requires an understanding of the processes causing observed major differences in charge equilibration between atomic and molecular projectiles, it has been shown that the typical consequence is a *negative* stopping-power enhancement.

An interesting aspect is the possibility of a clearing-the-way effect which deserves further study.

We have been able to qualitatively explain the main features in experimental data on the C_n-C system, in particular, the fact that major positive enhancements cannot be expected in the velocity range that has so far been accessible to experimental studies.

In connection with stopping data for aligned molecules we have also pointed at three pertinent competing effects, all of which predict the right order of magnitude, although none of them appears to fully explain the variation with projectile speed and dwell time.

ACKNOWLEDGMENTS

We would like to thank the staff and management of LSI, Palaiseau, in particular Professor A. Dunlop, for their hospitality during several visits at Ecole Polytechnique, and to Professor Y. Le Beyec and his colleagues for stimulating our interest in this aspect of particle penetration and providing access to unpublished information. Useful hints have been received from Professor L. C. Feldman and Dr. D. S. Gemmell. This work has been supported by a generous grant from Ecole Polytechnique to one of us (P. S.) and by the Danish Natural Science Research Council (SNF).

[1] Y. Le Beyec, Y. Hopillard, and H. Bernas, Nucl. Instrum. Methods Phys. Res. B **88**, 1 (1994).

[2] J. P. Thomas, *Correlated Effects in Atomic and Cluster Ion Bombardment and Implantation* [Nuclear Instrum. Methods Phys. Res. B **112** (1996)].

[3] K. Baudin, A. Brunelle, S. Della-Negra, D. Jacquet, P. Håkansson, Y. Le Beyec, M. Pautrat, R. R. Pinho, and C. Schoppmann, Nucl. Instrum. Methods Phys. Res. B **112**, 59 (1996).

[4] Y. Le Beyec, Int. J. Mass Spectrom. Ion Processes **174**, 101 (1998).

[5] H. Dammak, A. Dunlop, D. Leseur, A. Brunelle, S. Della-Negra, and Y. Le Beyec, Phys. Rev. Lett. **74**, 1135 (1995).

[6] N. A. Tahir, D. H. H. Hoffmann, J. A. Maruhn, and C. Deutsch, Nucl. Instrum. Methods Phys. Res. B **88**, 127 (1994).

[7] J. Matsuo, N. Toyoda, and I. Yamada, J. Vac. Sci. Technol. B **14**, 3951 (1996).

[8] I. Yamada, in *Application of Accelerators in Research and Industry*, Proceedings of the 14th International Conference, AIP Conf. Proc. No. 392 (AIP, NY, 1997), p. 479.

[9] P. Sigmund, I. S. Bitensky, and J. Jensen, Nucl. Instrum. Methods Phys. Res. B **112**, 1 (1996).

[10] W. Brandt, A. Ratkowski, and R. H. Ritchie, Phys. Rev. Lett. **33**, 1325 (1974).

[11] J. W. Tape, W. M. Gibson, J. Remillieux, R. Laubert, and H. E. Wegner, Nucl. Instrum. Methods **132**, 75 (1976).

[12] M. F. Steuer, D. S. Gemmell, E. P. Kanter, E. A. Johnson, and B. J. Zabransky, Nucl. Instrum. Methods Phys. Res. **194**, 277 (1982).

[13] E. Ray, R. Kirsch, H. H. Mikkelsen, J. C. Poizat, and J. Remillieux, Nucl. Instrum. Methods Phys. Res. B **69**, 133 (1992).

[14] K. Baudin *et al.*, Nucl. Instrum. Methods Phys. Res. B **94**, 341 (1994).

[15] C. Tomaschko, D. Brandl, R. Kügler, M. Schurr, and H. Voit, Nucl. Instrum. Methods Phys. Res. B **103**, 407 (1995).
[16] D. Ben-Hamu and D. Zajfman, Phys. Rev. A **56**, 4786 (1997).
[17] Z. L. Miskovic, W. W. Liu, and Y. N. Wang, Phys. Rev. A **58**, 2191 (1998).
[18] J. Steinbeck and K. Dettmann, J. Phys. C **11**, 2907 (1978).
[19] Y. N. Wang and T. C. Ma, Phys. Rev. A **50**, 3192 (1994).
[20] N. Bohr, Mat. Fys. Medd. K. Dan. Vidensk. Selsk. **18**(8), 1 (1948).
[21] H. Bethe, Ann. Phys. (Leipzig) **5**, 324 (1930).
[22] J. Lindhard, Mat. Fys. Medd. K. Dan. Vidensk. Selsk. **28 no. 8,** 1 (1954).
[23] K. Narumi, K. Nakajima, K. Kimura, M. Mannami, Y. Saitoh, S. Yamamoto, Y. Aoki, and H. Naramoto, Nucl. Instrum. Methods Phys. Res. B **135**, 77 (1998).
[24] N. Arista, Phys. Rev. B **18**, 1 (1978).
[25] G. Basbas and R. H. Ritchie, Phys. Rev. A **25**, 1943 (1982).
[26] J. Jensen, H. H. Mikkelsen, and P. Sigmund, Nucl. Instrum. Methods Phys. Res. B **88**, 191 (1994).
[27] F. Bloch, Ann. Phys. (Leipzig) **16**, 285 (1933).
[28] P. Sigmund, Phys. Rev. A **56**, 3781 (1997).
[29] N. Bohr, Philos. Mag. **25**, 10 (1913).
[30] M. F. Steuer and R. H. Ritchie, Nucl. Instrum. Methods Phys. Res. B **33**, 170 (1988).
[31] W. Brandt and M. Kitagawa, Phys. Rev. B **25**, 5631 (1982).
[32] M. Abramowitz and I. A. Stegun, *Handbook of Mathematical Functions* (Dover, New York, 1964).
[33] J. Oddershede and J. R. Sabin, At. Data Nucl. Data Tables **31**, 275 (1984).
[34] P. Sigmund and U. Haagerup, Phys. Rev. A **34**, 892 (1986).
[35] J. Lindhard and M. Scharff, Mat. Fys. Medd. K. Dan. Vidensk. Selsk. **27**, 1 (1953).
[36] J. C. Ashley, R. H. Ritchie, and W. Brandt, Phys. Rev. B **5**, 2393 (1992).
[37] J. Lindhard, Nucl. Instrum. Methods **132**, 1 (1976).
[38] A. Schinner and P. Sigmund, Nucl. Instrum. Methods Phys. Res. B (to be published).
[39] I. Abril, M. Vicanek, A. Gras-Marti, and N. R. Arista, Nucl. Instrum. Methods Phys. Res. B **67**, 56 (1992).
[40] F. J. Pérez-Pérez, I. Abril, N. Arista, and R. Garcia-Molina, Nucl. Instrum. Methods Phys. Res. B **115**, 18 (1996).
[41] P. Sigmund, Nucl. Instrum. Methods Phys. Res. B **115**, 111 (1996).
[42] O. B. Firsov, Zh. Eksp. Teor. Fiz. **36**, 1517 (1959) [Sov. Phys. JETP **36**, 1076 (1959)].
[43] G. J. Kumbartzki, G. Kroesing, H. Neuburger, W. Pietsch, and D. S. Gemmell, Ann. Isr. Phys. Soc. **4**, 163 (1981).
[44] D. Maor, P. J. Cooney, A. Faibis, E. P. Kanter, W. Koenig, and B. J. Zabransky, Phys. Rev. A **32**, 105 (1985).
[45] A. Brunelle, S. Della-Negra, J. Depauw, D. Jacquet, Y. Le Beyec, and M. Pautrat, Phys. Rev. A **59**, 4456 (1999).
[46] P. Sigmund, J. Phys. (Paris) **C2-50**, 175 (1989).
[47] V. I. Shulga, M. Vicanek, and P. Sigmund, Phys. Rev. A **39**, 3360 (1989).
[48] V. I. Shulga and P. Sigmund, Nucl. Instrum. Methods Phys. Res. B **47**, 236 (1990).
[49] K. Baudin, A. Brunelle, S. Della-Negra, J. Depauw, Y. Le Beyec, and E. S. Parilis, Nucl. Instrum. Methods Phys. Res. B **117**, 47 (1996).
[50] P. Sigmund and K. B. Winterbon, Nucl. Instrum. Methods **119**, 541 (1974).
[51] A. D. Marwick and P. Sigmund, Nucl. Instrum. Methods **126**, 317 (1975).
[52] M. F. Steuer, D. S. Gemmell, E. P. Kanter, E. A. Johnson, and B. J. Zabransky, IEEE Trans. Nucl. Sci. **NS-30**, 1069 (1983).
[53] M. F. Steuer, D. S. Gemmell, E. P. Kanter, E. A. Johnson, and J. Zabransky, Nucl. Instrum. Methods Phys. Res. B **13**, 137 (1986).
[54] M. F. Steuer and R. H. Ritchie, Nucl. Instrum. Methods Phys. Res. B **40/41**, 372 (1989).
[55] J. U. Andersen, G. C. Ball, J. A. Davies, W. G. Davies, J. S. Forster, J. S. Geiger, H. Geissel, and V. A. Ryabov, Nucl. Instrum. Methods Phys. Res. B **90**, 104 (1994).